

G. PERNA^{1,2}
M. LASTELLA¹
M. AMBRICO³
V. CAPOZZI^{1,2,✉}

Temperature dependence of the optical properties of ZnSe films deposited on quartz substrate

¹ Dipartimento di Scienze Biomediche dell'Università di Foggia, Viale L. Pinto, 71100 Foggia, Italy
² Istituto Nazionale di Fisica della Materia, Unità di Bari, Via Amendola 173, 70126 Bari, Italy
³ Istituto di Metodologie Inorganiche e dei Plasmi del C.N.R., via Orabona 4, 70126 Bari, Italy

Received: 14 July 2005 / Accepted: 23 November 2005
Published online: 26 January 2006 • © Springer-Verlag 2006

ABSTRACT ZnSe thin films were deposited by pulsed laser ablation on quartz substrate. The films were investigated by different characterization techniques, such as X-ray diffraction, Raman microspectroscopy, absorption, reflectivity, and photoluminescence spectroscopy. The XRD analysis showed the formation of cubic phase polycrystalline films. The Raman spectra confirmed the formation of ZnSe by the presence of TO and LO peaks at 202 cm^{-1} and 252 cm^{-1} , respectively. The analysis of absorption and reflectivity measurements permits evaluation of the band gap and excitonic energy at low temperature and the temperature dependence of the energy gap. The photoluminescence measurements indicated the possibility of obtaining intrinsic band-band radiative emission up to room temperature.

PACS 52.38.Mf; 78.55.-m; 78.55.Et

1 Introduction

ZnSe is a II–VI semiconductor with a direct band gap energy of about 2.7 eV at room temperature. Such a property makes ZnSe very interesting for optical devices emitting in the blue spectral region [1]. It is also used as window material in high efficiency solar cells, because its large band gap permits a large number of photons to reach the absorber layer [2]. High quality ZnSe thin films are usually grown by epitaxial techniques (such as MBE [3] and MOVPE [4]) on GaAs substrates because of the negligible lattice mismatch (0.27%) between these two semiconductors [4]. However, it is interesting to study the deposition of ZnSe films by means of simple and inexpensive techniques and using more commercially available substrates, in view of the low cost production of ZnSe based devices.

Many different techniques have recently been applied to the deposition of ZnSe films: electrodeposition [5], photochemical deposition [6], vacuum evaporation [7] and pulsed laser ablation (PLA) [8]. In particular, PLA is a very interesting and promising deposition technique, because it does not require ultrahigh vacuum pressure (as MBE and MOVPE) and

permits the congruent evaporation of Zn and Se and stoichiometric deposition of the ZnSe compound.

In the present paper we report on the optical properties of ZnSe films deposited by means of PLA technique onto commercially available quartz substrate. We remark that it is difficult to grow high quality ZnSe onto quartz substrate, due to the large lattice and thermal expansion coefficient mismatch between the two materials. The quality of the deposited films has been analysed by means of X-ray diffraction (XRD), Raman, absorption, reflectivity and photoluminescence (PL) techniques. The deposited films result in a polycrystalline and highly oriented film with a cubic structure. PL emission is observed from 20 K to room temperature. The analysis of the optical properties as a function of the temperature indicates that the radiative emission is due to band-band recombination.

2 Experimental

ZnSe films were grown on an amorphous quartz substrate by laser ablation of a ZnSe solid target. A frequency doubled Nd:Yag laser having a wavelength of 532 nm, a pulse width of 10 ns, a laser fluence of about 10 J/cm^2 and a repetition rate of 10 Hz was used as the pulsed laser source. The substrate was mounted on a rotating and heated holder, positioned 3 cm from the target. Film deposition was performed in an evacuated stainless steel chamber (residual pressure of 10^{-6} mbar). During the growth, the substrate temperature was kept at $400\text{ }^\circ\text{C}$ and the deposition time was 30 min. The ZnSe samples appeared adherent to the substrate. The thickness of a typical film was about 300 nm (measured by a profilometer).

The X-ray diffraction (XRD) analysis was performed by using the Cu K_α radiation ($\lambda = 1.5406\text{ \AA}$) from a conventional θ – 2θ diffractometer.

The Raman spectra were measured at room temperature by means of a Raman confocal microspectrometer using the 488 nm line of an Ar ion as laser source and a notch filter (200 cm^{-1} line-width) to suppress the scattered laser light. The Raman signal was detected by means of a cooled ($T = 223\text{ K}$) CCD and recorded on a personal computer. The laser beam was focused, by an Olympus optical microscope with a $\times 100$ objective, on the ZnSe film, obtaining an illuminated spot of about $1\text{ }\mu\text{m}$ diameter. Raman spectra recorded from several points on the film surface were very similar to each

✉ Fax: +39 0881 745387, E-mail: v.capozzi@unifg.it

other, indicating sample homogeneity. The laser power on the sample surface was about 0.1 mW. The mean spectral resolution was 4 cm^{-1} .

Absorption and reflectivity measurements were performed by using a 100 W tungsten lamp as the light source. The samples were mounted in a He-closed cycle refrigerator thermoregulated from 20 K to 300 K. The light transmitted and reflected from the sample was analysed by means of a double grating spectrometer (1 meV/mm of dispersion) and detected by a GaAs cooled ($-20 \text{ }^\circ\text{C}$) photomultiplier. Photon counting technique was used to record the spectra. As for the PL measurements, the 325 nm line of a He-Cd laser was used for exciting the sample in the standard backscattering geometry. The light emitted from the sample surface was analysed and detected by the same apparatus used for absorption and reflectivity measurements.

3 Results and discussion

The XRD spectrum of the ZnSe film deposited on quartz substrate is shown in Fig. 1. It can be observed that the XRD pattern shows a prominent peak at 27.2 degrees, corresponding to the diffraction from the (111) plane. No other XRD peak is evident in the scanned angular range.

The lattice plane spacing d can be calculated by the Bragg formula $d = \lambda / 2 \sin \theta$ [9], where λ is the X-ray wavelength and θ is the Bragg angle; it results in $d = 3.2759 \text{ \AA}$. The lattice parameter a is determined for a cubic structure by the following expression [9]:

$$\frac{1}{d^2} = \frac{(h^2 + k^2 + l^2)}{a^2} \quad (1)$$

where h, k, l represent the Miller indexes of the lattice planes. By considering that $h, k, l = 1, 1, 1$ for the ZnSe film, a lattice parameter value $a = 5.6740 \text{ \AA}$ is obtained. This value is in good agreement with that reported in the literature ($a = 5.6687 \text{ \AA}$ [10]).

The full width at half maximum (FWHM) of the observed XRD peak is about 0.38° . Such a value can be used for calculating the average crystalline size D , using the Debye–Scherrer relationship $D = 0.9\lambda / (\text{FWHM}) \cos \theta$ [11]. The obtained D value is $21 \pm 2 \text{ nm}$. Therefore, the ZnSe film is polycrystalline and grows highly oriented with zincblende structure.

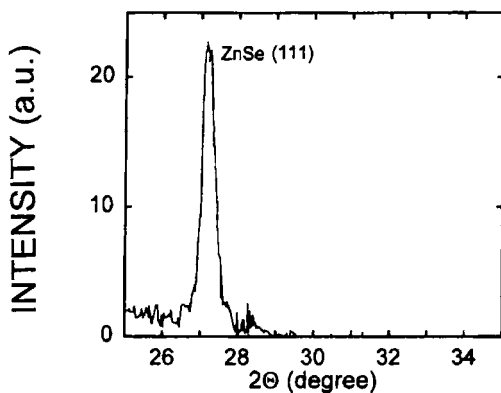


FIGURE 1 XRD spectrum of a ZnSe film deposited on quartz substrate

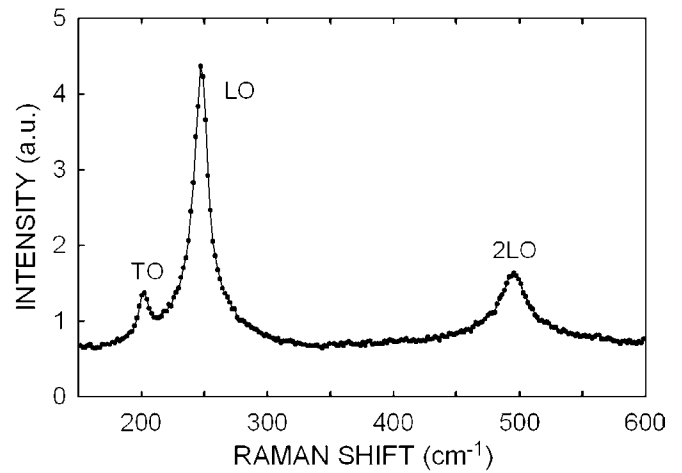


FIGURE 2 Raman spectrum of a ZnSe film deposited on quartz substrate. The attribution of the peak to TO, LO phonons is reported

Figure 2 shows a Raman spectrum of a ZnSe film, where the intense peak at 252 cm^{-1} can be attributed to the longitudinal optical (LO) phonon mode of ZnSe [10]. The presence of such a feature confirms the formation of a ZnSe lattice with crystalline quality. The peaks at about 202 cm^{-1} and 500 cm^{-1} are due to transversal optical (TO) phonon mode and to the replica of the LO phonon mode (2LO), respectively.

Figure 3 shows the absorption (dots), reflectivity (triangles) and PL (dashed line) spectra at $T = 20 \text{ K}$ of a ZnSe film in the near band gap region. The reflectivity spectrum is characterized by a dispersion line with a well defined dip: it can be assigned to the free excitonic resonance, in agreement with the analysis performed in [4]. In the same spectral range, the absorption coefficient spectrum shows a monotonic increase versus energy and no spectral features. Therefore, we deduce that the absorption curve is due to band-band transition, with no excitonic contribution. The PL spectrum is characterized by a broad peak centred at 2.765 eV . The attribution of such a PL band can be clarified if the excitonic and band gap energies are known. Therefore, in order to obtain the excitonic energy value of the ZnSe film we have fitted the experimental reflectivity data to a model which takes into account the presence of a surface layer depleted of excitons (dead layer), as described in [12, 13]. According to this model, the spectral reflectivity $R(E)$ can be expressed by the following expression:

$$R(E) = rr^*, \quad r = \frac{r_{12} + r_{23}e^{2i\theta}}{1 + r_{12}r_{23}e^{2i\theta}} \quad (2)$$

with $\theta = 2\pi d / \lambda_m$, where λ_m is the light wavelength within the medium, d is the thickness of the dead layer, $r_{12} = (1 - \varepsilon_s^{1/2}) / (1 + \varepsilon_s^{1/2})$ is the reflection coefficient at the air-dead layer boundary, $r_{23} = (\varepsilon_s^{1/2} - \tilde{n}) / (\varepsilon_s^{1/2} + \tilde{n})$ is the reflection coefficient at the layer-bulk boundary, ε_s is the background dielectric constant ($\varepsilon_s = 8.3$ for ZnSe [9]), $\tilde{n} = n + ik$ is the complex refractive index, whose real (n) and imaginary (k) parts are related to the real (ε_1) and imaginary (ε_2) parts of the dielectric function $\varepsilon = \varepsilon_1 + i\varepsilon_2$ by the following equations.

$$n(\omega) = \left\{ \frac{1}{2} \left[\varepsilon_1(\omega) + (\varepsilon_1^2(\omega) + \varepsilon_2^2(\omega))^{1/2} \right] \right\}^{1/2} \quad (3a)$$

$$k(\omega) = \left\{ \frac{1}{2} \left[-\varepsilon_1(\omega) + (\varepsilon_1^2(\omega) + \varepsilon_2^2(\omega))^{1/2} \right] \right\}^{1/2} . \quad (3b)$$

The dielectric function $\varepsilon = \varepsilon_1 + i\varepsilon_2$ can be represented, in the damped harmonic oscillator model [14], by the expression:

$$\varepsilon(\omega) = \varepsilon_\infty + \frac{A\omega_0^2}{\omega_0^2 - \omega^2 - i\omega\Gamma} \quad (4)$$

where ε_∞ is the background dielectric constant for $\omega \rightarrow \infty$ ($\varepsilon_\infty = 5.6$ for ZnSe [10]), A is the polarizability, Γ a broadening parameter and $\omega_0 = E_0/\hbar$ the circular frequency corresponding to the exciton energy E_0 .

The fit parameters were the excitonic frequency ω_0 , the broadening parameter Γ , the dead layer thickness d and the polarizability A . The (2) describes quite well the experimental data, as can be seen in Fig. 3 (continuous line along R plot) and yields an excitonic energy of 2.7477 ± 0.0002 eV. This value is lower with respect to the excitonic energy of ZnSe single crystals (2.801 eV [10]). Such red shift is related to the lattice mismatch and the difference in the thermal expansion coefficient between the film and substrate, which result in a shrinkage of the band gap. An estimate of the energy gap E_g value can be obtained by analysing the absorption spectrum in Fig. 3 according to the Elliot theory [15, 16], by considering the contribution of the continuum interband transition:

$$\alpha(E) \propto C \int_{E_g}^{\infty} dE \frac{1}{1 - e^{-2\pi z}} \frac{\Gamma_c}{(E - E_g)^2 + \Gamma_c^2} \quad (5)$$

where $z^2 = R/(E - E_g)$, R is the Rydberg energy, C and Γ_c are an amplitude and broadening parameter, respectively. The performed fit is illustrated in Fig. 3 (continuous line over α plot). By considering C , E_g and Γ_c as fitting parameters (R has been fixed to 20 meV [10]), we have obtained an E_g value of 2.7702 ± 0.0006 eV. Such a value is lower than the literature value of the energy gap of ZnSe single crystal (2.820 eV [10]) for the same reasons discussed above. Therefore, the PL band can be attributed to band-band recombination. The excitonic recombination is lacking because local electric fields related to structural disorder dissociate excitonic complexes.

PL spectra at different temperature are reported in Fig. 4. It can be seen that the intensity of the band-band emission decreases with increasing temperature, due to the increase of thermally activated nonradiative recombination mechanisms. Nonetheless, the intrinsic PL emission persists up to room temperature.

In order to obtain the temperature dependence of the energy gap, we have performed and analysed the absorption measurements at different temperature from 20 K to 300 K. Some of these measurements are illustrated in Fig. 5a (points), with the fit (continuous line) to (5) in the near band gap region. The reflectivity measurements have also been performed and analysed at different temperatures, in order to obtain the temperature dependence of the excitonic energy. However, we believe that the analysis with (2) better reproduces the experimental data for lower temperatures

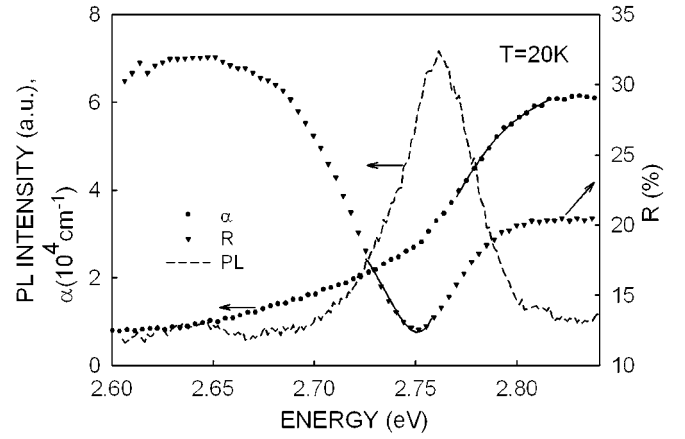


FIGURE 3 Absorption coefficient (dots), reflectivity (triangles) and PL (dashed line) spectra of a ZnSe film at $T = 20$ K. The continuous lines are least squares fit of the absorption and reflectivity data to (5) and (2), respectively. The arrows indicates the vertical axis (left for absorption coefficient and PL spectra, right for reflectivity spectrum) which is related to each spectrum

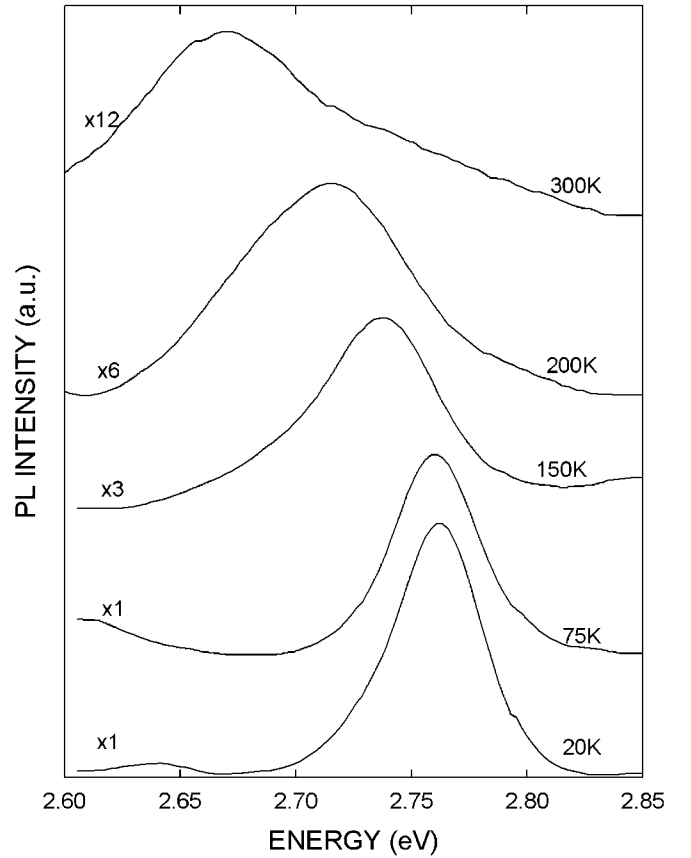


FIGURE 4 PL spectra at different temperatures of a ZnSe film deposited on quartz substrate

than for larger ones, because of the thermal dissociation of excitons. Therefore, we have analysed (continuous line) the reflectivity data (points) up to 100 K, as illustrated in Fig. 5b.

The energy gap presents a red shift and broadening as the temperature increases, due to electron-phonon interaction [17]. The equation (5) fits the experimental data well in the near band gap region for all the examined temperatures.

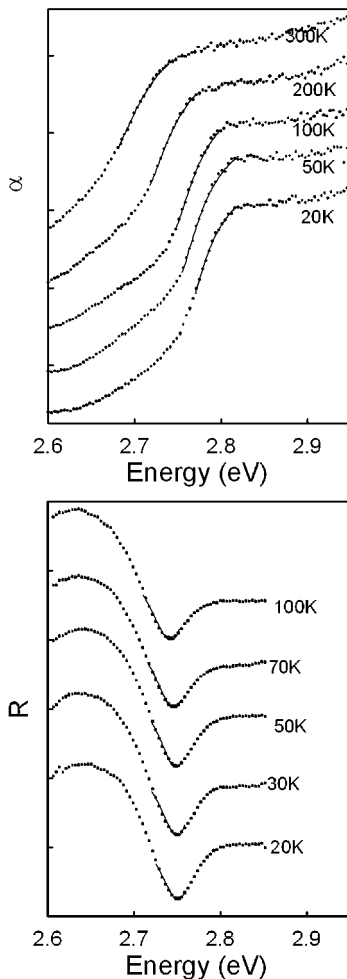


FIGURE 5 Absorption (a) and reflectivity (b) spectra of a ZnSe film at different temperatures. The continuous lines are least squares fit of the absorption and reflectivity data to (5) and (2), respectively

The obtained E_g values are shown in Fig. 6 (points). These data have been fitted (continuous line) by means of a Bose–Einstein expression, usually used to describe the thermal red shift of the energy gap $E_g(T)$ [17]:

$$E_g(T) = E_g(0) - \frac{2a_B}{\exp\left(\frac{\theta}{T}\right) - 1} \quad (6)$$

where a_B represents the strength of the electron–phonon interaction and θ is a temperature corresponding to the average energy of the phonons involved in the process. The equation (6) fits well to the E_g values as a function of the temperature. The value obtained for θ parameter (214 ± 24 K) is lower than the θ corresponding to LO phonons (350 K). This suggests the contribution of both acoustical and optical phonons to the shrinkage of the band gap.

4 Conclusion

We have reported on the structural and optical properties of ZnSe films deposited onto quartz substrate by

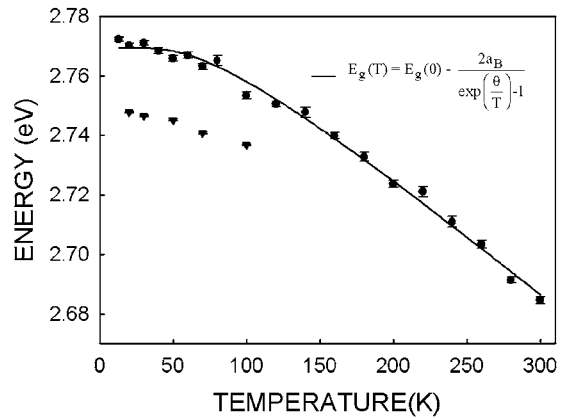


FIGURE 6 Temperature dependence of the band gap (circles) and excitonic (triangles) energies of a ZnSe film deposited on quartz substrate. The band gap and excitonic energies have been obtained by fitting of the experimental absorption and reflectivity spectra to (5) and (2), respectively. The continuous line is the best fit of the band gap data to (6). The obtained values of the fitting parameters are: $E(0) = 2.770 \pm 0.001$ eV; $a_B = 0.043 \pm 0.006$ eV; $\theta = 214 \pm 24$ K

means of PLA technique. The ZnSe films grow polycrystalline and highly oriented, although the large lattice and thermal expansion coefficient mismatch between the film and the substrate. The crystalline quality is indicated both by a quite narrow XRD peak and by the presence of well resolved LO and TO peaks in the Raman spectrum. The absorption and reflectivity measurements yield the band gap and excitonic energies, which result lower than the literature value of ZnSe single crystals. This result is related to the strain caused by the lattice mismatch. The presence of intrinsic band-band emission in the PL spectra from low temperature to room temperature indicates the good optical quality of the deposited films.

REFERENCES

- 1 M. Godlewski, E. Guziewicz, K. Kooalko, E. Lusakowska, E. Dynowska, M.M. Godlewski, E.M. Godys, M.R. Phillips, J. Lumin. **102–103**, 455 (2003)
- 2 A.M. Chaparro, M.A. Martinez, C. Guillen, R. Bayon, M.T. Gutierrez, J. Herrero, Thin Solid Films **361–362**, 177 (2000)
- 3 S.Z. Wang, S.F. Yoon, L. He, X.C. Shen, J. Appl. Phys. **90**, 2314 (2001)
- 4 A.L. Gurskii, Y.P. Rakovich, E.V. Lutsenko, A.A. Gladyschuk, G.P. Yablonskii, H. Hamadeh, M. Heuken, Phys. Rev. B **61**, 10314 (2000)
- 5 S. Soundeswaran, O. Senthil Kumar, R. Dhanasekaran, P. Ramasamy, R. Kumaresan, M. Ichimura, Mater. Chem. Phys. **82**, 268 (2003)
- 6 R. Kumaresan, M. Ichimura, E. Arai, Thin Solid Films **414**, 25 (2002)
- 7 S. Vankatachalam, D. Mangalaraj, S.K. Narayandass, K. Kim, J. Yi, Physica B **358**, 27 (2005)
- 8 N. Xu, B.H. Boo, J.K. Lee, J.H. Kim, J. Phys. D: Appl. Phys. **33**, 180 (2000)
- 9 C. Kittel, *Introduction to Solid State Physics* (Wiley, NY 1971)
- 10 Landolt Boernstein Tables, Vols. 17a and b, O. Madelung (Ed.), M. Schulz, H. Weiss (Springer, Berlin 1982)
- 11 H.P. Klug, L.E. Alexander, *X-ray Diffraction Procedures* (Wiley, NY 1954)
- 12 F. Evangelista, J.U. Fischbach, A. Frova, Phys. Rev. B **9**, 1516 (1974)
- 13 F. Evangelista, A. Frova, F. Patella, Phys. Rev. B **10**, 4253 (1974)
- 14 J. Langois, Phys. Rev. B **16**, 1699 (1977)
- 15 R.J. Elliot, Phys. Rev. **108**, 1383 (1957)
- 16 A.R. Goñi, A. Cantarero, K. Syassen, M. Cardona, Phys. Rev. B **41**, 10111 (1990)
- 17 L. Viña, S. Logothetidis, M. Cardona, Phys. Rev. B **30**, 1979 (1984)